

1 **Zero-baseline Analysis of GPS/BeiDou/Galileo Between-**
2 **Receiver Differential Code Biases (BR-DCBs): Time-wise**
3 **Retrieval and Preliminary Characterization**

4
5

B. Zhang¹ and P.J.G. Teunissen^{1,2}

6 ¹*GNSS Research Centre, Curtin University, Perth, Australia*

7 ²*Geoscience and Remote Sensing, Delft University of Technology, Delft, The Netherlands*

8
9

ABSTRACT

10

11 When sensing the Earth’s ionosphere using multiple Global Navigation Satellite Systems (GNSSs) special care needs to be
12 taken of the receiver Differential Code Bias (DCB) contributions to the error budget. For this reason timely and accurate
13 retrieval of multi-GNSS receiver DCBs with the goal of gaining insight into their characteristics would be of relevance. In this
14 contribution we propose a method that is able to time-wisely retrieve the Between-Receiver DCBs (BR-DCBs) from code
15 measurements collected by a zero-baseline setup, thereby eliminating most common error sources. We base our investigations
16 on dual-frequency GPS (L1+L2), BeiDou (B1+B2) and Galileo (E1+E5a) measurements collected in 2013 with a 30 second
17 sampling rate by four multi-GNSS receivers of three types connected to one common antenna. For each receiver-pair, we
18 determine the time-wise estimates of GPS/GEO/IGSO/MEO/Galileo BR-DCBs from the corresponding code measurements.
19 With the use of statistical hypothesis testing schemes, we confirm that: (1). the time-wise estimates of BR-DCBs for all tested
20 receiver-pairs exhibit good intra-day stability; and (2). the daily weighted average (DWA) estimates of GEO/IGSO/MEO BR-
21 DCBs are inconsistent for receiver-pairs of mixed type, due to the presence of BeiDou code Inter-Satellite-Type-Biases
22 (ISTBs). We also identify likely factors accounting for the variability in the DWA estimates of BR-DCBs over a 1-year
23 interval as: (1). receiver firmware upgrades; and (2). daily maximum temperature variations at receiver sites.

24
25

Keywords: GPS, BeiDou, Galileo, Between-Receiver Differential Code Bias (BR-DCB), Inter-Satellite-Type-Bias (ISTB)

26
27

1 INTRODUCTION

2
3 The space-borne and ground-based Global Navigation Satellite System (GNSS) measurements with extensive spatial coverage
4 and high temporal resolution are particularly ideal for studying the ionosphere [1]. Over the past few decades, the ionospheric
5 information retrieved from the GPS measurements broadcast at two frequencies has enabled us to understand the intrinsic
6 mechanisms of the space weather effects [2, 3], to explore the potential causes of the seismic hazards [4, 5], and to improve the
7 empirical precision of space geodetic applications [6-8]. In addition to the GPS that is undergoing uninterrupted modernization,
8 the Chinese BeiDou and the European Galileo are currently under development for global operation as well [9]. For the period
9 covered by this study (Jan.-Dec. 2013), the BeiDou constellation consisting of 14 satellites in orbit (five GEO + five IGSO +
10 four MEO) has become operational in the Asian-Pacific region [10], whilst the Galileo is still in the deployment phase and has
11 four In-Orbit-Validation (IOV) satellites operating [11]. In a multi-GNSS context, one would be able to acquire much deeper
12 insight into the actual state of the ionosphere than before [12, 13].

13 Precise estimation of vertical Total Electron Content ($vTEC$) parameters from dual- or multi-frequency GNSS
14 measurements is a crucial prerequisite for GNSS-based ionosphere studies [14]. For this purpose one has to tackle the
15 Differential Code Bias (DCB) contributions to the error budget [15]. Despite the evidence in [16, 17], it is still a prevalent rule-
16 of-thumb to separate the DCBs into those introduced by the satellite and those introduced by the receiver. The near constant
17 space environment onboard the GNSS constellation usually gives rise to fairly promising long-term stability of the satellite
18 DCBs [18, 19], especially for those satellites under normal operating condition. As a consequence, one would be able to
19 determine the estimable satellite DCBs with relatively high precision [20] and thus get rid of their impact on the estimated
20 $vTEC$ easily [21, 22]. In contrast, however, receiver DCBs may experience significant short-term variation during a time
21 period of one day or even a few hours. One possible reason, among others, is due to the changing temperature conditions at the
22 receiver antenna, along the cable, or in the internal receiver hardware [23, 24]. Such temporal variability of receiver DCBs, if
23 not circumvented properly, will partially account for both the levelling errors underlying the line-of-sight ionospheric
24 observables [25], as well as the $vTEC$ modelling errors [26-28].

25 With the ultimate goal of improving the reliability of $vTEC$ estimation, so far a variety of approaches have been proposed
26 to determine the characteristics (typically the stability) of the receiver DCBs retrieved either from the $vTEC$ estimation process
27 as a by-product [29, 30], or from differencing the ionospheric observables determined for two co-located receivers [25, 31].
28 However, for the following two reasons these approaches may still be inadequate. First, when using such methods the retrieved
29 receiver DCBs may still be affected by un-modelled biases. Second, the so-obtained time series of receiver DCBs are usually
30 of low time resolution (a few hours to one day) and may thus fail to identify any possible receiver DCB variations over shorter

1 time intervals (e.g. less than 1 hour).

2 In this contribution, we first develop an approach for retrieving Between-Receiver DCBs (BR-DCBs) based on a zero-
3 baseline set up. Without relying on the vTEC estimation process or the formation of ionospheric observables, our approach is
4 able to achieve time-wise BR-DCB retrieval by employing only a single epoch of between-receiver, between-frequency
5 double-differenced (DD) GNSS code measurements. Since for zero-baseline most common error sources can be largely
6 cancelled out in the DD code measurements [32], the error budgets affecting our BR-DCB retrieval are thereby minimized.
7 With the use of GPS/BeiDou/Galileo measurements collected in 2013 with a sampling rate of 30 seconds by four multi-GNSS
8 receivers connected to one common antenna, we will investigate: (1). the intra-day stability in the time-wise BR-DCB
9 estimates; (2). the consistency between the daily weighted average (DWA) estimates of GEO/IGSO/MEO BR-DCBs for a
10 common receiver-pair; (3). the main factors accounting for the inter-day variability in the DWA estimates of BR-DCBs.

11

12 **METHOD DESCRIPTION**

13

14 In this section, we outline the procedure of our time-wise BR-DCB retrieval approach. Next to that, we briefly illustrate two
15 statistical hypothesis testing schemes that are adopted to validate the intra-day stability in time-wise BR-DCB estimates and
16 the consistency between DWA estimates of GEO/IGSO/MEO BR-DCBs.

17

18 **Time-wise Retrieval of BR-DCBs**

19

20 Let us assume that, at certain epoch i , two receivers forming a zero-baseline are able to simultaneously track a number of
21 GNSS satellites at two frequencies. Concerning one of the satellites s , its between-receiver single-differenced (SD) code
22 observation equations take the form

$$23 \quad E\{p_j^{s,G}(i)\} = dt^G(i) + b_j^G(i) \quad (1)$$

24 where $E\{\cdot\}$ denotes the expectation operator, $j=1,2$ denotes the frequency index, $p_j^{s,G}(i)$ denotes the dual-frequency SD
25 code measurements for satellite s that belongs to GNSS constellation G transmitting code division multiple access (CDMA)
26 signals. Unknown parameters are: $dt^G(i)$ the SD receiver clock, $b_j^G(i)$ the frequency-dependent SD receiver code biases.

27 The system of observation equations represented by (1) is not solvable, since all the unknown parameters are not
28 individually estimable. For this reason we further difference the SD code observation equations between two frequencies and
29 eventually get

$$E\{p_{12}^{s,G}(i)\} = b_{12}^G(i) \quad (2)$$

where $p_{12}^{s,G}(i) = p_1^{s,G}(i) - p_2^{s,G}(i)$ is the DD code measurement and $b_{12}^G(i) = b_1^G(i) - b_2^G(i)$ is the BR-DCB parameter of our interest.

The formal precision of $p_{12}^{s,G}(i)$ can be given as

$$D\{p_{12}^{s,G}(i)\} = \left[\frac{2\sigma^{s,G}}{\sin\{\theta^{s,G}(i)\}} \right]^2 \quad (3)$$

where $D\{\cdot\}$ is the dispersion operator, $\sigma^{s,G}$ denotes the zenith-referenced undifferenced code standard deviation, and $\theta^{s,G}(i)$ denotes the elevation angle of satellite s at epoch i . For the multi-GNSS code measurements collected by the receivers involved in this study, the empirically determined values of $\sigma^{s,G}$ have been made available in [33, 34].

At every epoch, after incorporating the functional model similar to (2) and the stochastic model similar to (3) for all the satellites belonging to one common constellation, we can readily retrieve the BR-DCB estimates, along with their formal precision, using the least-square estimator. The epoch-wise least-square solution is therefore a weighted average over all satellites, in which the reciprocal value of (3) is used as weighting.

We remark that, when applying the BR-DCB retrieval approach described above to BeiDou code measurements, one should be aware of the possible presence of the code Inter-Satellite-Type-Biases (ISTBs) for receiver-pairs of mixed type [35]. By definition, the BeiDou code ISTBs associated with two satellite types, denoted as $B_j^{gm}(i)$, can be interpreted as

$$B_j^{gm}(i) = b_j^g(i) - b_j^m(i) \quad (4)$$

where $b_j^g(i)$ ($b_j^m(i)$) denotes the SD receiver code biases involved in the SD code observation equations formulated for satellite type g (m).

Further differencing $B_j^{gm}(i)$ at two frequencies will yield the following identity

$$B_1^{gm}(i) - B_2^{gm}(i) = [b_1^g(i) - b_2^g(i)] - [b_1^m(i) - b_2^m(i)] \quad (5)$$

where $b_1^g(i) - b_2^g(i)$ and $b_1^m(i) - b_2^m(i)$ are in fact the BeiDou BR-DCBs retrieved by DD code measurements belonging to satellite types g and m , respectively. From (5) it follows that, would dual-frequency BeiDou code ISTBs be present and different, one may have to retrieve satellite type dependent BeiDou BR-DCBs.

Finally, it is worth mentioning that our time-wise BR-DCB retrieval approach is unlikely to benefit from further involvement of the carrier-phase measurements. Usually, this fact holds true in the case where the real-valued ambiguity parameters are estimated (ambiguity-float scenario). Moreover, even if the (between-receiver, between-satellite) DD ambiguity

1 parameters have been successfully resolved into integers (ambiguity-fixed scenario), the contribution of incorporating carrier-
 2 phase measurements to the BR-DCB retrieval is still virtually negligible [36].

3

4 **Statistical Hypothesis Testing**

5

6 With one day's time-wise BR-DCB estimates available, the DWA estimate of them, denoted as \bar{b}_{12}^G , can be calculated as
 7 follows

$$8 \quad \bar{b}_{12}^G = \frac{\sum_{i=1}^t b_{12}^G(i) / \sigma_{b_{12}^G}^2(i)}{\sum_{i=1}^t 1 / \sigma_{b_{12}^G}^2(i)} \quad (6)$$

9 where t is the number of epochs, $b_{12}^G(i)$ is weighted according to its formal precision $\sigma_{b_{12}^G}^2(i)$.

10 In addition, with the use of error propagation law, we can also obtain the formal precision of \bar{b}_{12}^G which is denoted as $\sigma_{\bar{b}_{12}^G}^2$
 11 and reads

$$12 \quad \sigma_{\bar{b}_{12}^G}^2 = \frac{1}{\sum_{i=1}^t 1 / \sigma_{b_{12}^G}^2(i)} \quad (7)$$

13 It is remarked that computation of $b_{12}^G(i)$ and $\sigma_{b_{12}^G}^2$ as given above will form the basis for our illustration of two statistical
 14 hypothesis testing schemes in the following.

15 Test statistic T_s used to diagnose the intra-day stability of $b_{12}^G(i)$ can be constructed as

$$16 \quad T_s = \sum_{i=1}^t \frac{(b_{12}^G(i) - \bar{b}_{12}^G)^2}{\sigma_{b_{12}^G}^2(i)} \quad (8)$$

17 where T_s is Chi-square distributed with $t-1$ degrees of freedom, assuming that $b_{12}^G(i)$ is normally distributed. The critical
 18 value of T_s can be written as $\chi_{\alpha_s}^2(t-1, 0)$ in which the level of significance is set to α_s . One would conclude that $b_{12}^G(i)$ does
 19 not exhibit any significant changes over time if $T_s < \chi_{\alpha_s}^2(t-1, 0)$ occurs.

20 At the same time, in order to ascertain the possible dependency of BeiDou BR-DCBs upon the satellite type, we construct
 21 the following test statistic T_c which reads

$$22 \quad T_c = \frac{\bar{b}_{12}^g - \bar{b}_{12}^m}{\sqrt{\sigma_{\bar{b}_{12}^g}^2 + \sigma_{\bar{b}_{12}^m}^2}} \quad (9)$$

1 where \bar{b}_{12}^g (\bar{b}_{12}^m) denote the DWA estimate of $[b_1^g(i) - b_2^g(i)]$ ($[b_1^m(i) - b_2^m(i)]$), while its formal precision is given as $\sigma_{\bar{b}_{12}^g}^2$
 2 ($\sigma_{\bar{b}_{12}^m}^2$). T_c has a standard normal distribution. One would decide for a significant difference between \bar{b}_{12}^g and \bar{b}_{12}^m if
 3 $|T_c| > N_{0.5\alpha_c}(0,1)$ holds for a given significance level α_c .

4

5 EXPERIMENTAL ANALYSIS

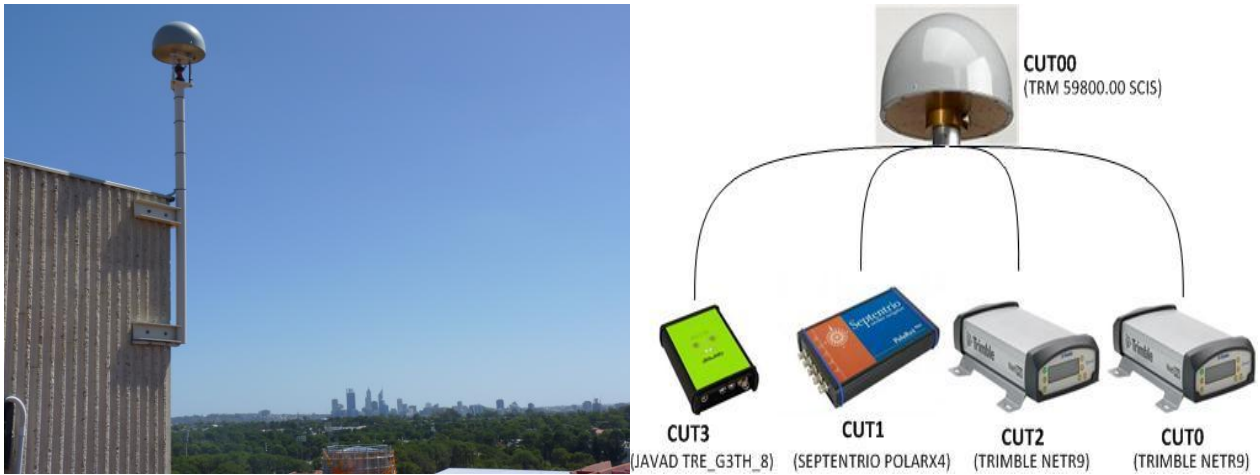
6

7 Data Preparation and Processing

8

9 The experimental data sets are measured by four multi-GNSS receivers from the GPS, the BeiDou and the Galileo
 10 constellations in 2013 with a sampling rate of 30 seconds and a cut-off elevation angle of 15 degrees. All the receivers are
 11 placed in a cabinet located in the roof-top plant room of Building 402 at the main campus of Curtin University (Perth). They
 12 are commonly connected to one antenna mounted on the roof of the same building (see Fig. 1). Table 1 presents an overview of
 13 the basic characteristics of the receivers and antenna, while Table 2 summarizes the features of the code measurements used.

14



15

16

17 **Figure 1.** Curtin GNSS geodetic grade antenna (*CUT00*) and four multi-GNSS receivers of three types used in this study. *Left:*
 18 antenna setup with SCIS radome. *Right:* receiver–antenna connectivity

19

20 We define three independent receiver-pairs, all referring to the *CUT0* as pivot receiver. We time-wisely retrieve the
 21 GPS/GEO/IGSO/MEO/Galileo BR-DCBs using the corresponding code measurements on a per receiver-pair basis. We
 22 emphasize here again that, to investigate the possible dependency of BeiDou BR-DCBs upon the satellite type, the code

1 measurements from BeiDou GEO/IGSO/MEO satellites are processed separately, as if they were from three different
 2 constellations.

3 We derive the epoch-wise satellite positions that are fundamental inputs to elevation angle computation from the
 4 broadcast ephemerides. We remark that, receiving broadcast ephemerides from BeiDou (Galileo) constellation by at least one
 5 of our experimental receivers becomes possible only after day 49 (17) of 2013. When we compute the critical value for test
 6 statistic T_s (T_c), the level of significance α_s (α_c) is chosen equal to 5%.

7

8

Table 1. Four experimental multi-GNSS receiver characteristics

Receiver name	Receiver type	Antenna type	Remark
CUT0 (<i>pivot</i>)	Trimble NETR9	TRM59800.00 SCIS	Firmware version was upgraded from 4.70 to 4.80 at day 175, 2013
CUT1	Septentrio PolaRx4		
CUT2	Trimble NETR9		The same firmware upgrade process as CUT0
CUT3	Javad TRE_G3TH_8		Removed during days 242-246 and 254-261, 2013

9

10

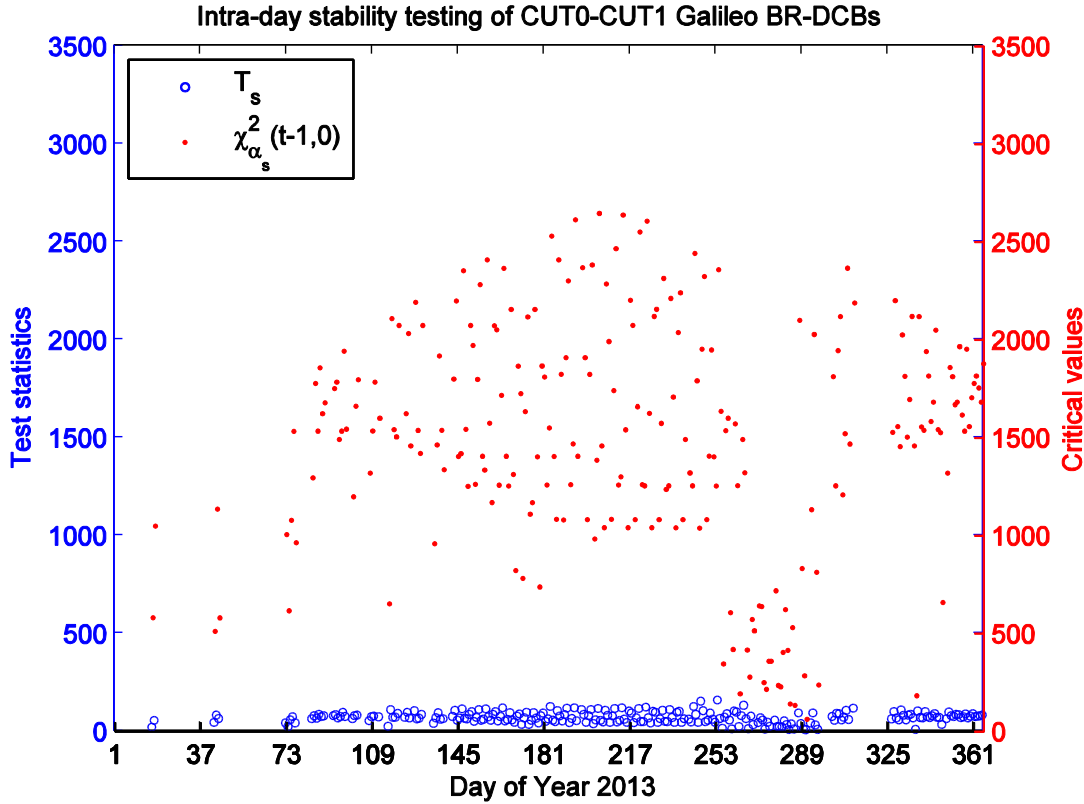
Table 2. Overview of dual-frequency, multi-GNSS code measurements used in this study

Constellation	Band	Frequency (MHz)	Component
GPS	L1	1575.42	C
	L2	1227.60	W
BeiDou	B1	1561.098	I
	B2	1207.14	I
Galileo	E1	1575.42	X: CUT0, CUT3
			C: CUT1, CUT2
	E5a	1176.45	X: CUT0, CUT3 Q: CUT1, CUT2

1
2
3
4
5
6

We shall for the sake of brevity restrict our presentation to a selected set of representative BR-DCB results. All conclusions drawn about the characteristics of the presented BR-DCBs hold true for the rest of our BR-DCB results as well.

Analysis of Intra-day Stability in Time-wise BR-DCB Estimates



7
8

Figure 2. Test statistics T_s (blue circles) used to diagnose the intra-day stability in the time-wise estimates of CUT0-CUT1 Galileo BR-DCBs. Critical values $\chi_{\alpha_s}^2(t-1,0)$ (red dots) computed using level of significance $\alpha_s = 5\%$, together with the degree of freedom $(t-1)$

12
13
14
15
16

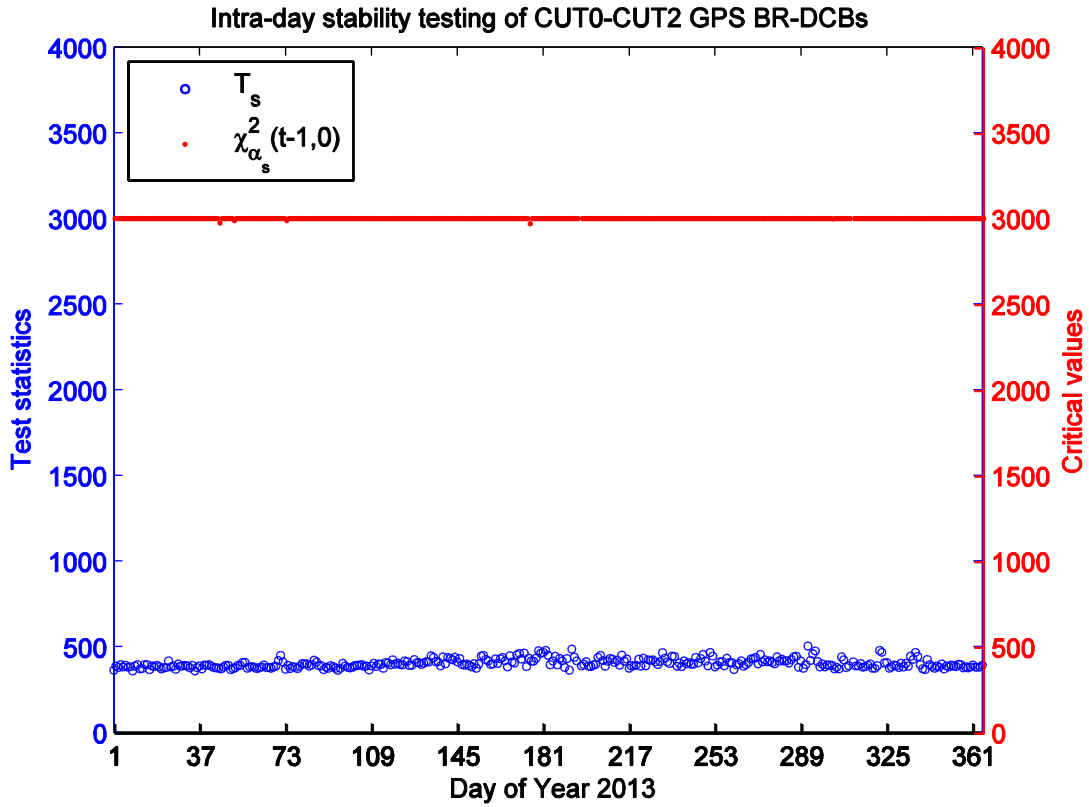
We first test the time-wise Galileo BR-DCB estimates for receiver-pair CUT0-CUT1 (*Trimble-Septentrio*). Figure 2 depicts a series of test statistics T_s (blue circles) along with their critical values $\chi_{\alpha_s}^2(t-1,0)$ (red dots) computed for all testing days. A few gaps present in the time series of T_s correspond to the time periods without navigation ephemerides (e.g. days 1-17) or lack of visible IOV satellites above cut-off elevation angle. Due to the fact that we assign a fixed value (5%) to α_s , the values

1 of $\chi_{\alpha_s}^2(t-1,0)$ are thereby solely driven by the degree of freedom $(t-1)$ and may vary dramatically from day to day. For
2 those days (e.g. 253-289) when only one IOV satellite is intermittently visible the values taken by $\chi_{\alpha_s}^2(t-1,0)$ can drop down
3 to 500 or even smaller. Clearly, it follows here that $T_s < \chi_{\alpha_s}^2(t-1,0)$ always holds true for all the testing days and thus can be
4 taken as indication of intra-day stability in the time-wise BR-DCB estimates considered here.

5 Likewise, Figure 3 presents the testing results for the time-wise GPS BR-DCB estimates for another receiver-pair CUT0-
6 CUT2 (*Trimble-Trimble*). Contrary to Fig. 2 in which the $\chi_{\alpha_s}^2(t-1,0)$ values vary remarkably between days, it follows here
7 that the $\chi_{\alpha_s}^2(t-1,0)$ values stay almost constant over the entire one year period, mainly due to the nearly invariant $(t-1)$
8 ranging from 2850 to 2879. Again, we see from Fig. 3 that, the computed values of T_s (<500) are always significantly smaller
9 than that of $\chi_{\alpha_s}^2(t-1,0)$ (>3000). This confirms that the time-wise BR-DCB estimates tested here are sufficiently stable over
10 every single day of 2013.

11 We remark that our test statistics T_s only have a chi-square distribution if the BR-DCB estimators are normally
12 distributed. We verify this by displaying first of all the time-wise Galileo BR-DCB estimates retrieved at day 211 (an arbitrary
13 choice) as a histogram in Fig. 4 (*subplot a*), which has 2354 samples and 40 bins of width 0.15 ns. Also, we depict therein the
14 empirical probability density function (PDF) of $N(0.26,0.57)$ as a red curve, which corresponds to the empirical mean (0.26
15 ns) and the empirical standard deviation (0.57 ns) of those samples. Generally, we can recognize from subplot (a) that the
16 histogram fits reasonably well with the empirical normal PDF, thereby implying the BR-DCB estimates retrieved at this day
17 closely obey a normal distribution. However, we have to point out that, the histogram seems to be slightly asymmetric as these
18 estimates are heterogeneous in their formal precision. Furthermore, we use the Quantile-Quantile (QQ) plot (*subplot b*) as
19 another tool to graphically demonstrate the close-to-normality of samples depicted in subplot (a). In such a QQ plot, the
20 ordered samples are plotted against the quantiles of the empirical normal distribution $N(0.26,0.57)$. In accord with what we
21 have learnt from subplot (a), the linearity of the blue crosses shown in subplot (b) also suggests that the samples are close-to-
22 normally distributed.

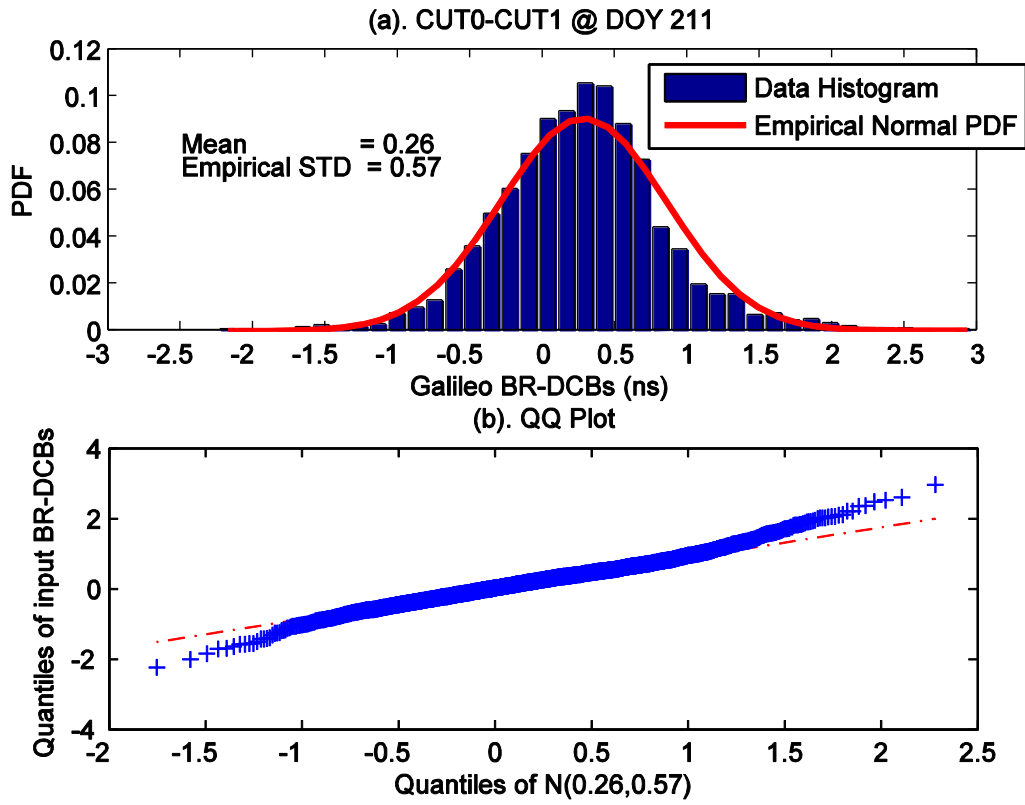
23



1
2
3
4
5
6
7
8
9
10
11
12
13
14

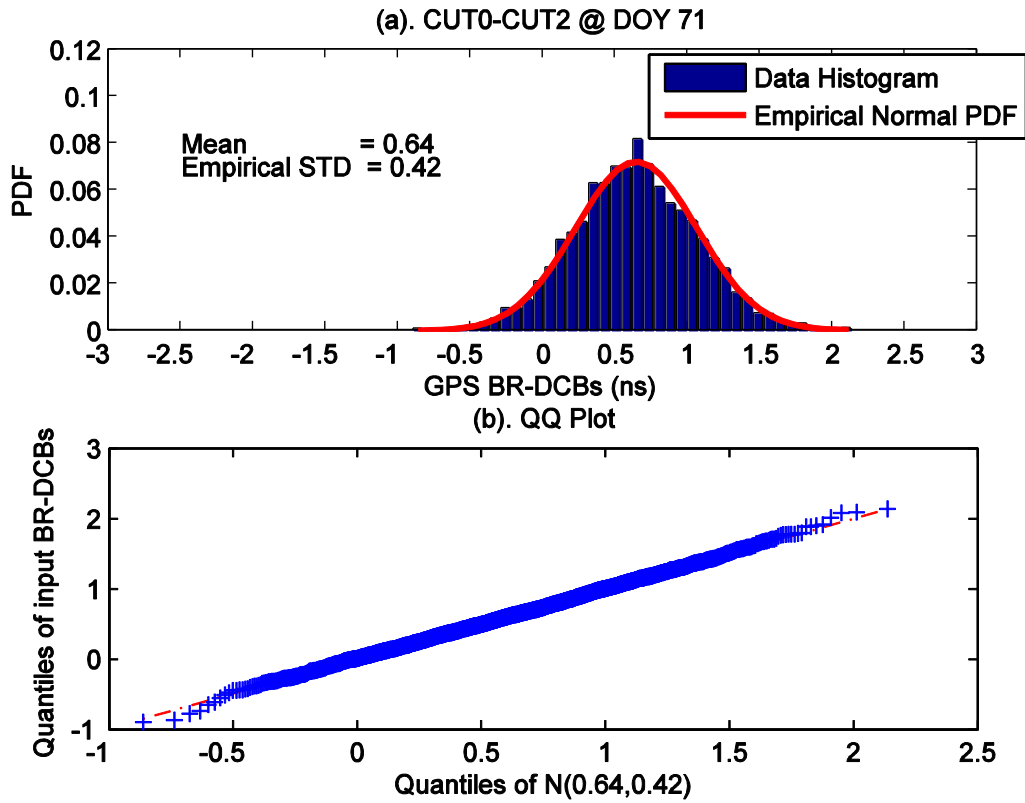
Figure 3. Test statistics T_s (blue circles) used to diagnose the intra-day stability in the time-wise estimates of CUT0-CUT2 GPS BR-DCBs. Critical values $\chi_{\alpha_s}^2(t-1,0)$ (red dots) computed using level of significance $\alpha_s = 5\%$, together with the degree of freedom $(t-1)$

Additionally, we address in Fig. 5 the histogram of time-wise GPS BR-DCB estimates retrieved at day 71 (subplot a) as well as the corresponding QQ plot (subplot b). Considering first the subplot (a), the histogram has a total of 2880 samples and 40 bins of width 0.15 ns. The empirical normal PDF, determined by the empirical mean (0.64 ns) and the empirical standard deviation (0.42 ns) of these samples, is depicted as a red curve. In contrast to what we see from subplot (a) of Fig. 4, the conformity between the histogram and the empirical normal PDF becomes more evident. Moreover, since these BR-DCB estimates are more homogeneous in their formal precision the histogram is less asymmetric. With respect to the QQ plot depicted in subplot (b), the linearity of green crosses confirms the normal distribution of the samples as well.



1
2
3
4
5
6
7

Figure 4. *Panel (a):* The histogram of time-wise Galileo BR-DCB estimates referring to day 211 and receiver-pair of CUT0-CUT1: 2354 samples and 40 bins of width 0.15 ns, and the empirical theoretical normal distribution (*red curve*) based on the mean (*0.26 ns*) and empirical standard deviation (*0.57 ns*) of the samples. *Panel (b):* QQ plot of samples versus normal distribution $N(0.26,0.57)$



1

2

3

4

5

6

7

8

9

10

11

12

13

14

15

16

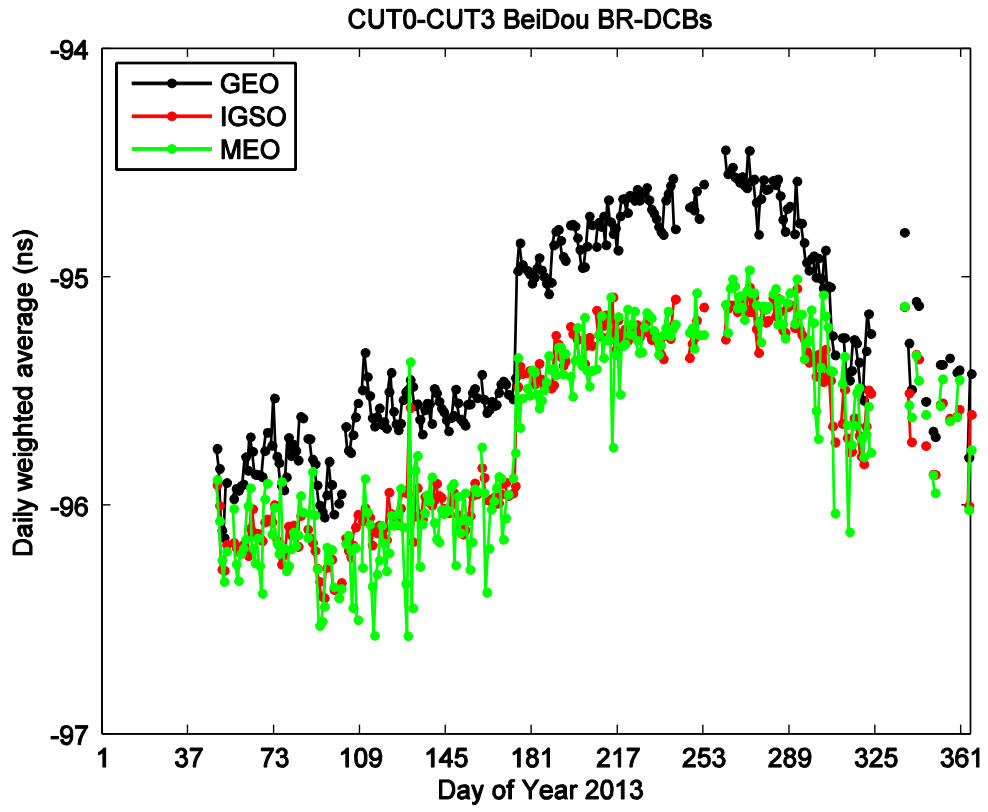
17

Figure 5. *Panel (a):* The histogram of time-wise GPS BR-DCB estimates referring to day 71 and receiver-pair of CUT0-CUT2: 2880 samples and 40 bins of width 0.15 ns, and the empirical theoretical normal distribution (*red curve*) based on the mean (*0.64 ns*) and empirical standard deviation (*0.42 ns*) of the samples. *Panel (b):* QQ plot of samples versus normal distribution $N(0.64, 0.42)$

Possible Dependency of BeiDou BR-DCB Estimates upon Satellite Type

As inferred from (5), the BeiDou BR-DCBs would become dependent on satellite type, provided that the dual-frequency code ISTBs are present and in the meantime differ from each other. We will verify this finding here by means of investigating the consistency between the DWA estimates of GEO/IGSO/MEO BR-DCBs retrieved for two receiver-pairs, involving not only the CUT0-CUT3 of mixed type (*Trimble-Javad, ISTB-affected*), but the CUT0-CUT2 of common type (*Trimble-Trimble, ISTB-free*) as well. We further remark that for CUT0-CUT3 the empirical values of dual-frequency BeiDou code ISTBs were already published in [35] (*cf. Table 5 therein*). This, therefore, makes it possible for us to “predict” the offsets between any two of GEO/IGSO/MEO BR-DCBs for this receiver-pair using (5). We will compare these “predicted” offsets with their “computed” counterparts determined from our BeiDou BR-DCB estimates for cross-checking purpose.

1



2

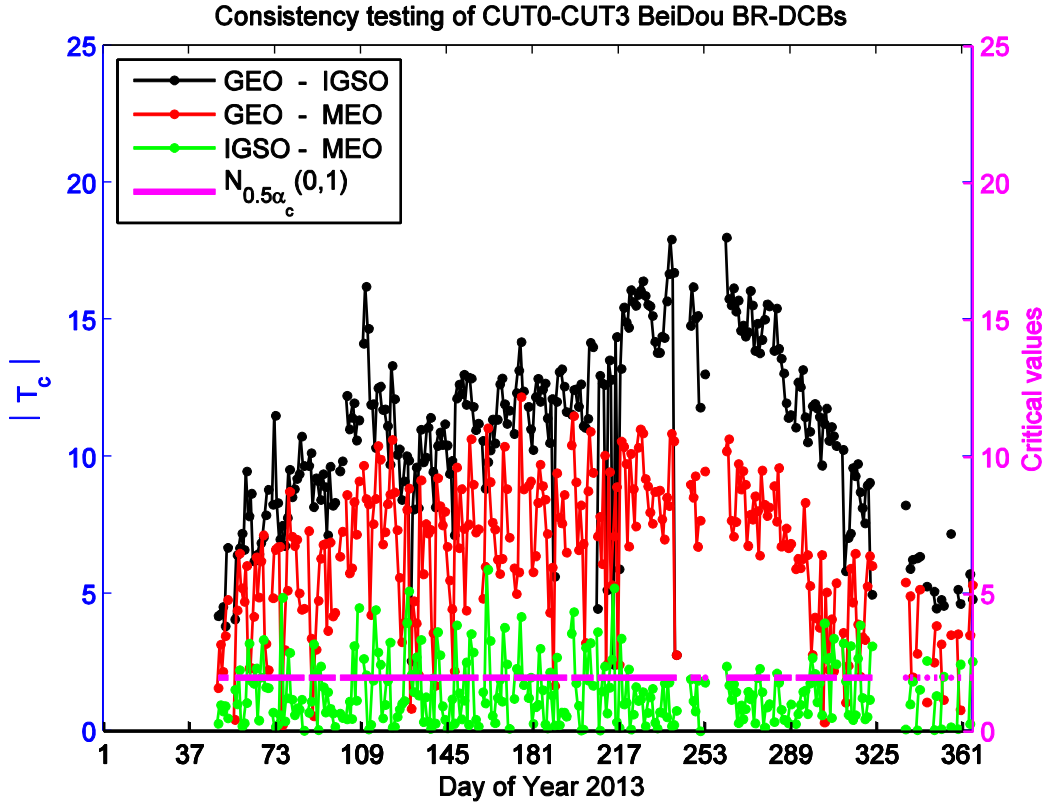
3

4 **Figure 6.** The DWA estimates of CUT0-CUT3 (*Trimble-Javad*) BeiDou BR-DCBs in 2013: GEO results (*black dotted line*),

5 IGSO results (*red dotted line*) and MEO results (*green dotted line*)

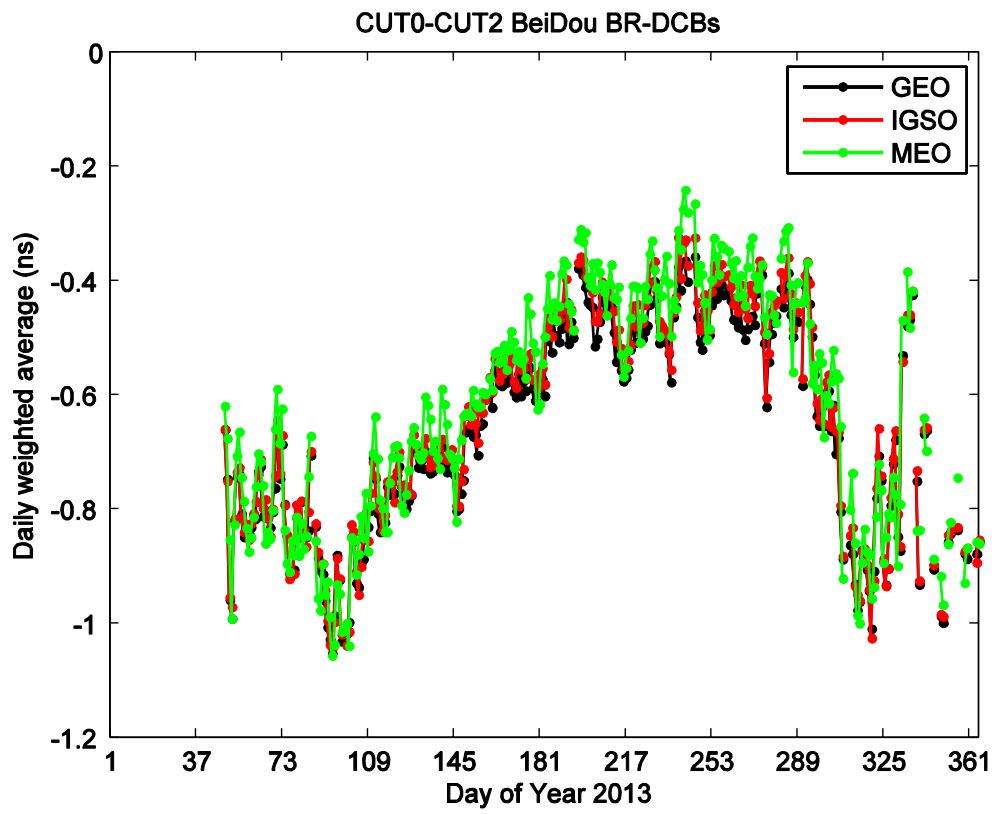
6

7



1
2
3 **Figure 7.** Test statistics $|T_c|$ (*black/red/green dotted lines*) used to diagnose the consistency between CUT0-CUT3
4 GEO/IGSO/MEO BR-DCB estimates (*cf. Fig. 6*). Critical value $N_{0.5\alpha_c}(0,1)$ (*magenta line*) computed using level of
5 significance $\alpha_c = 5\%$
6

7 We show in Fig. 6 the DWA estimates of GEO/IGSO/MEO BR-DCBs retrieved for CUT0-CUT3. It follows that, the
8 IGSO BR-DCB time series (*dotted red line*) are generally in good agreement with MEO BR-DCB ones (*dotted green line*). The
9 mean value of their offsets amounts to -0.02 ns (-0.6 cm), which is very close to the predicted value of -1 cm as derived from
10 [35]. In contrast to the other two, the GEO BR-DCB time series (*dotted black line*) are found to have a constant offset of
11 roughly 0.45 ns (13.5 cm), which deviates slightly from the corresponding predicted value of 9 cm as derived from [35].
12 According to [37], the difference between the GEO and non-GEO BR-DCBs might result from the fact that GEO satellites are
13 essentially fixed in the sky for a static receiver. Because of this, geometry-dependent errors such as multipath tend to introduce
14 a constant bias in observations from GEO satellites. This GEO-specific bias depends on the multipath sensitivity of each
15 receiver (i.e. receiver dependent) and will not completely cancel out by taking between-receiver single-differencing. Therefore,
16 one should be aware that the BeiDou code ISTBs may lead to inconsistent GEO/IGSO/MEO BR-DCB estimates.
17



1
2
3
4
5
6
7

Figure 8. The DWA estimates of CUT0-CUT2 (*Trimble-Trimble*) BeiDou BR-DCBs in 2013: GEO results (*black dotted line*), IGSO results (*red dotted line*) and MEO results (*green dotted line*)

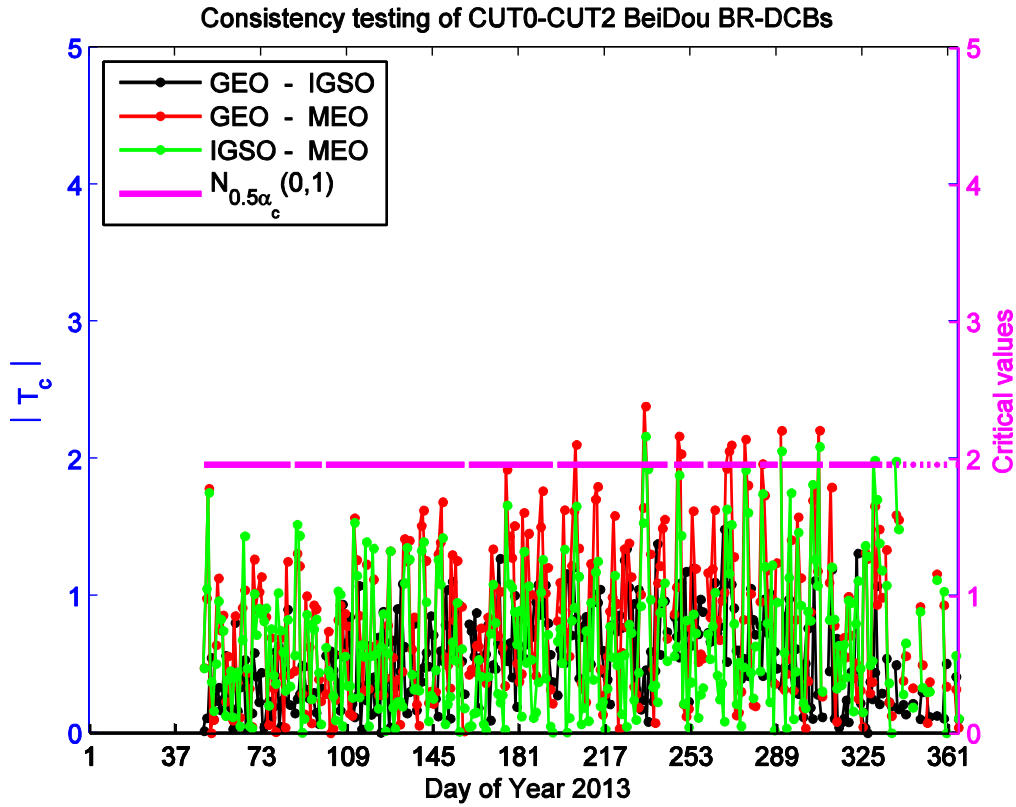


Figure 9. Test statistics $|T_c|$ (black/red/green dotted lines) used to diagnose the consistency between CUT0-CUT2 GEO/IGSO/MEO BR-DCB estimates (cf. Fig. 8). Critical value $N_{0.5\alpha_c}(0,1)$ (magenta line) computed using level of significance $\alpha_c = 5\%$

With the use of (9), we test whether the offsets between any two of the time series given in Fig. 6 are statistically significant or not. For each day we compute three test statistics T_c and present their absolute values $|T_c|$ in Fig. 7. Also, critical values $N_{0.5\alpha_c}(0,1)$ ($=1.96$) remaining constant over all testing days are depicted as a magenta line. From Fig. 7 the inconsistency between GEO and non-GEO BR-DCBs again follows, as those computed values of $|T_c|$ depicted as black and red dotted lines always exceed 1.96.

We show in Fig. 8 the DWA estimates of GEO/IGSO/MEO BR-DCBs retrieved for CUT0-CUT2. Due to the fact that this receiver-pair is not subject to BeiDou code ISTBs, the three time series start to be fairly consistent. This finding can be further verified by testing results presented in Fig. 9, in which the computed values of $|T_c|$ are below 1.96 with quite rare exceptions.

In summary, the discussions above might allow us to draw a very preliminary conclusion: when retrieving the BeiDou

1 BR-DCBs for receiver-pairs of mixed type, one should take special care of the effect due to the code ISTBs that may be
2 present. Provided that the dual-frequency code ISTBs deviates significantly from each other, it then requires one to consider
3 the dependency of BeiDou BR-DCBs upon satellite type. On the other hand, one can safely introduce satellite type independent
4 BeiDou BR-DCBs for receiver-pairs of common type.

6 **Analysis of Inter-day Variability in BR-DCB Estimates**

8 Although we did not mention it yet, one may recognize from Fig. 6 that an abrupt change occurs in the DWA estimates of
9 CUT0-CUT3 BeiDou BR-DCBs before day 181, and from Fig. 8 that there is an apparent trend in the DWA estimates of
10 CUT0-CUT2 BeiDou BR-DCBs. We will attempt to seek for the possible reasons behind such two phenomena. Before doing
11 so, we present in Table 3 the statistics of the DWA estimates of BR-DCBs retrieved for all three receiver-pairs over 2013, in
12 which the empirical standard deviation values would provide us an overall impression on the inter-day variability of each
13 group of BR-DCB estimates. In general it follows from Table 3 that, with respect to a common constellation, the BR-DCB
14 estimates retrieved for two receiver-pairs of mixed type (in particular CUT0-CUT3) always have larger empirical standard
15 deviations than those for receiver-pair of common type (CUT0-CUT2), thus implying more evident inter-day variability. In
16 addition to CUT0-CUT3 whose BeiDou BR-DCB results have been previously discussed, we see for CUT0-CUT1 the
17 inconsistent mean values of GEO/IGSO/MEO BR-DCB estimates as well. This can also be attributed to the BeiDou code
18 ISTBs that are found to be present for this receiver-pair.

19 After taking a closer look at Fig. 6, we find that the abrupt change occurs at day 175 and its size is about 0.5 ns. This
20 situation holds true as well for the BeiDou BR-DCB results obtained for CUT0-CUT1 as shown in Fig. 10. We identify the
21 firmware upgrade undergone by receiver CUT0 at day 174 as the possible reason. This is because, in general, the receiver code
22 biases depend not only on the hardware, but also on the digital signal processing that may change with a firmware version
23 upgrade [37]. Interestingly, from Fig. 8 we do not see the occurrence of such an abrupt change in CUT0-CUT2 BeiDou BR-
24 DCB estimates from day 175 onwards. This is due to the fact that, both receivers involved are of common type and have
25 experienced identical firmware upgrade process (see Table 1). Consequently, the changes in both receivers' absolute DCBs
26 after upgrading the firmware are very likely the same and thus cannot be reflected in the BR-DCB estimates.

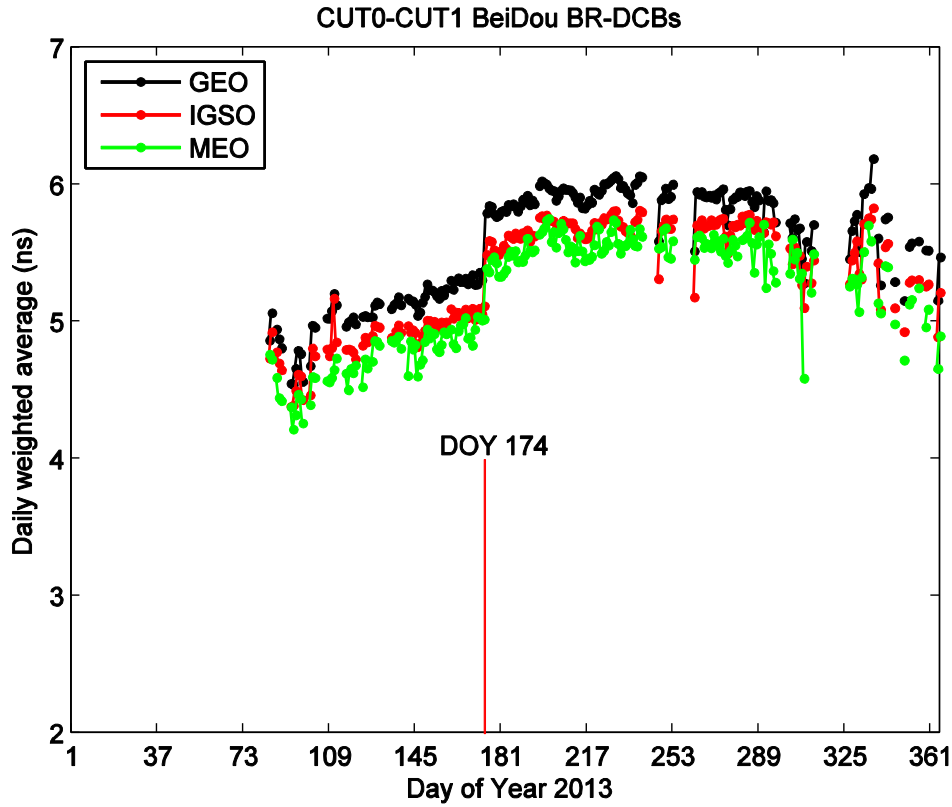
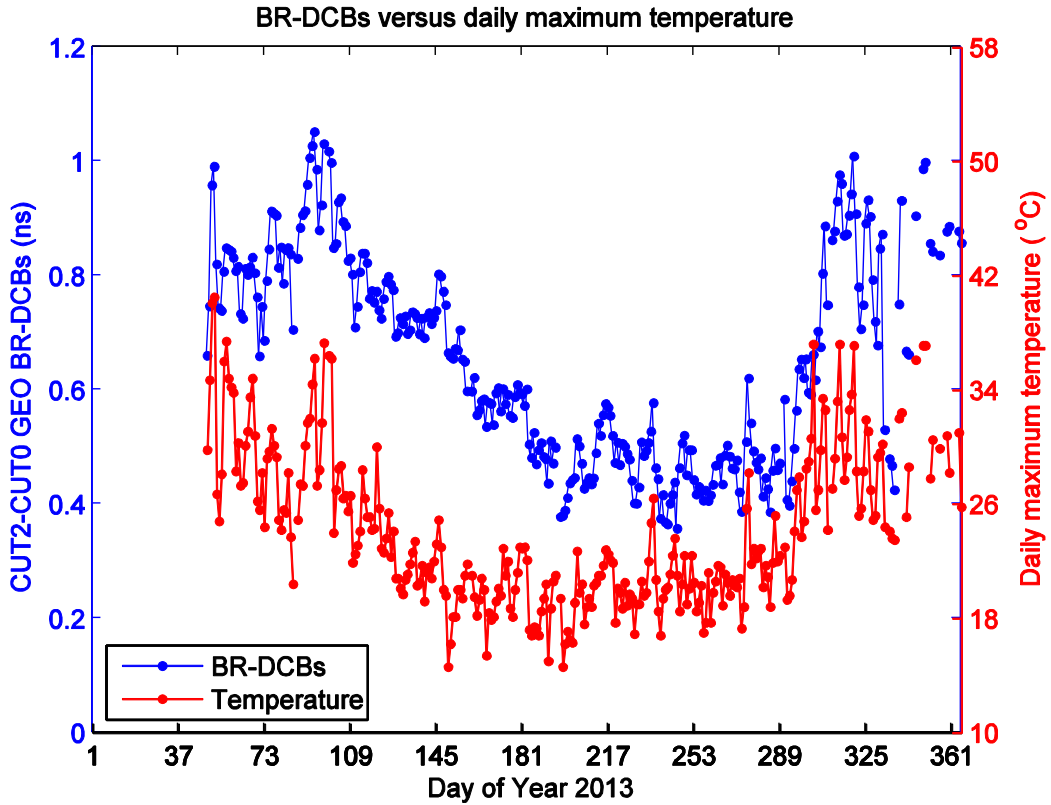


Figure 10. The DWA estimates of CUT0-CUT1 (*Trimble-Septentrio*) BeiDou BR-DCBs in 2013: GEO results (*black dotted line*), IGSO results (*red dotted line*) and MEO results (*green dotted line*). Only after day 84, CUT1 starts to receive signals from BeiDou IGSO and MEO satellites. The vertical red line indicates the day (174) when the firmware version of CUT0 was upgraded from 4.70 to 4.80

According to the literature devoted to GNSS (albeit GPS-only) receiver DCB studies (e.g. [23, 24, 31, 38, 39]), the temperature effect is generally acknowledged as a predominant factor accounting for receiver DCB variations. With this in mind, we assume that the inter-day variability in DWA estimates of CUT0-CUT2 BeiDou BR-DCBs (*cf. Fig. 8*) is a direct consequence of varying temperature conditions between days. To verify our assumption, we depict in Fig. 11 the time series of CUT2-CUT0 GEO BR-DCB estimates (*dotted blue line*), together with that of daily maximum temperature (*dotted red line*) observed by a weather station deployed about 8 km away from our receiver sites. We determine the Pearson correlation coefficient (r) between the two time series to quantify their statistical dependence. For a statistical sample size greater than 100, as is the case here, the absolute value of r greater than 0.254 is rated significant. Here the computed Pearson r value is equal to 0.79 and the corresponding p-value for testing the null hypothesis of no correlation against the alternative that there is a nonzero correlation is fairly small (≈ 0). This shows that both time series are highly correlated and it thus suggests that the

1 inter-day variability in BR-DCB estimates is indeed due to the temperature effect. During an almost 1-year period, the response
 2 of BR-DCB estimates to the temperature variations is rather moderate in this case: the peak-to-peak variation between the
 3 highest and the lowest BR-DCB estimates is only about 0.6 ns.

4



5

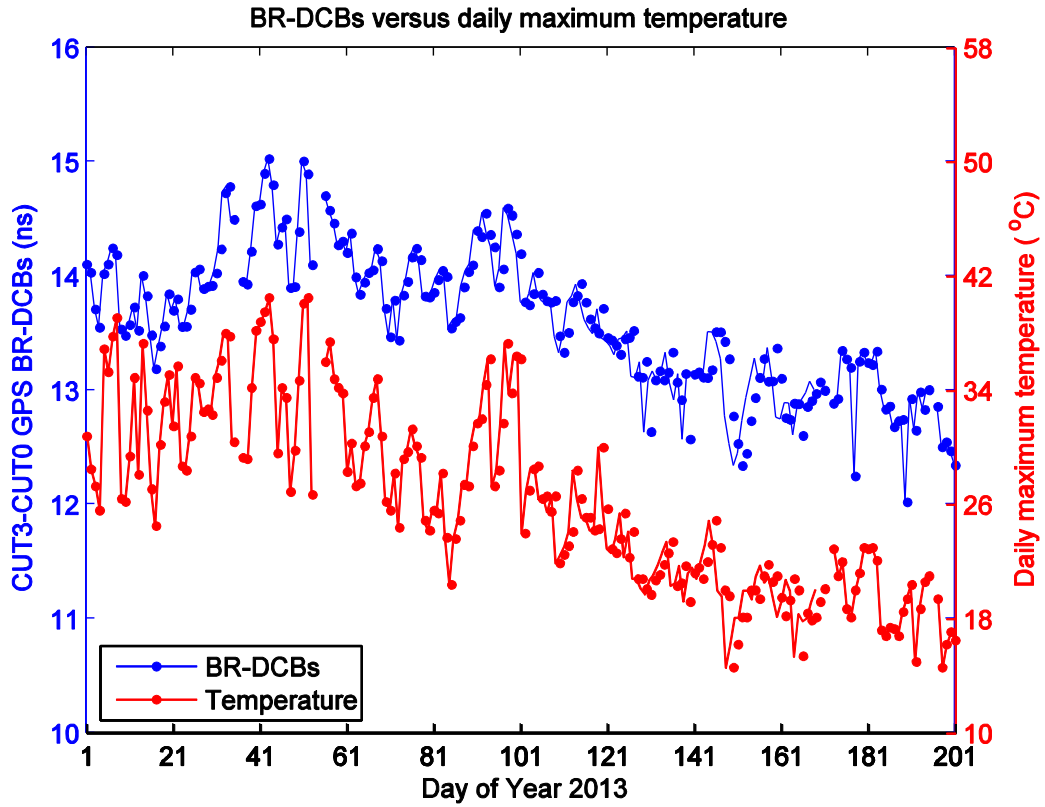
6

7 **Figure 11.** The DWA estimates of CUT2-CUT0 GEO BR-DCBs (*blue dotted line*) and the daily maximum temperature
 8 values (*red dotted line*) measured by a weather station deployed about 8 km away from the receiver site. The Pearson
 9 correlation coefficient between both time series is 0.788 with a corresponding p-value of almost zero

10

11 Recall that there exist three likely factors accounting for the receiver DCB dependence on temperature: the antenna, the
 12 cable and the receiver hardware [23]. For our zero-baseline setup, the cables can further be separated into one antenna-splitter
 13 cable commonly shared by all the receivers, as well as those splitter-receiver cables connecting the splitter to each receiver.
 14 One reason for having temperature effect zero-baseline BR-DCB estimates might be caused by reflections in the cables that
 15 depend on the antenna impedance and can slightly vary with temperature. Since the radio frequency paths along the cables to
 16 the two receivers are not exactly identical, these reflections would induce a different code bias on both receivers [37].

17



1
2
3 **Figure 12.** The DWA estimates of CUT3-CUT0 GPS BR-DCBs (*blue dotted line*) and the daily maximum temperature
4 values (*red dotted line*) measured by a weather station deployed about 8 km away from the receiver site. The time period
5 indicated by the horizontal axis covers days 1-201 of 2013. The Pearson correlation coefficient between both time series is
6 0.90 with a corresponding p-value very close to zero

7
8 We further show in Fig. 12 the CUT3-CUT0 GPS BR-DCB estimates, as well as the daily maximum temperature for the
9 first 201 days of 2013. The Pearson r value computed between two time series is now as great as 0.9. This again clearly
10 demonstrates that the inter-day variability of BR-DCB estimates can be linked to temperature effect. Compared to Fig. 11,
11 although the time period considered here covers only 201 days, the peak-to-peak variation of BR-DCB estimates is however
12 more considerable now and can reach roughly 3 ns. This fact suggests that the temporal variability of BR-DCB estimates
13 induced by temperature varies from receiver-pair to receiver-pair, which needs to be taken into consideration in future
14 modelling efforts.

Table 3. Statistics of the DWA estimates of BR-DCBs over 2013: mean/empirical standard deviation (ns)

Receiver-pair	GPS	BeiDou			Galileo
		GEO	IGSO	MEO	
CUT0-CUT1 (Trimble-Septentrio)	-13.63/0.36	5.45/0.49	5.32/0.43	5.19/0.44	0.18/0.25
CUT0-CUT2 (Trimble-Trimble)	0.52/0.16	-0.65/0.18	-0.64/0.19	-0.62/0.20	0.35/0.11
CUT0-CUT3 (Trimble-Javad)	-13.13/0.82	-95.24/0.47	-95.67/0.40	-95.69/0.46	-12.88/1.80

SUMMARY AND CONCLUSIONS

In this contribution, we described a method for time-wise retrieval of BR-DCBs employing code measurements simultaneously collected by two receivers forming one zero-baseline from GNSS constellations transmitting CDMA signals. These time-wise estimates of the BR-DCBs have therefore the same high temporal resolution as the collected GNSS measurements. We described two statistical hypothesis testing schemes with the goal of testing, respectively, the intra-day stability of time-wise estimates of the BR-DCBs and the consistency between the DWA estimates of the GEO/IGSO/MEO BR-DCBs.

We carried out a field campaign over an entire 1-year period (2013) at the main campus of Curtin University in Bentley (Perth), during which, dual-frequency GPS/BeiDou/Galileo measurements were collected by four receivers of three types connected to one common antenna, with a sampling rate of 30 seconds. We defined three independent receiver-pairs and for each of them we retrieved the time-wise estimates of GPS/GEO/IGSO/MEO/Galileo BR-DCBs. The main conclusions drawn from analyzing these BR-DCB estimates include:

- For each group of BR-DCB estimates, they are sufficiently stable over a 1-day period;
- For receiver-pairs of mixed type, possible inconsistency between GEO/IGSO/MEO BR-DCB estimates may occur, mainly due to the effect of BeiDou code ISTBs;
- The DWA estimates of BR-DCBs may exhibit an abrupt change induced by receiver firmware upgrades, whose size can reach about 0.5 ns;
- The variability in the DWA estimates of BR-DCBs over an almost 1-year period shows a high correlation with the daily maximum temperature variations.

1 **ACKNOWLEDGMENTS**

2

3 This work has been executed in the framework of the Positioning Program Project 1.01 "New carrier phase processing
4 strategies for achieving precise and reliable multi-satellite, multi-frequency GNSS/RNSS positioning in Australia" of the
5 Cooperative Research Centre for Spatial Information (CRC-SI). This work was also partially funded by the CAS/KNAW joint
6 research project 'Compass, Galileo and GPS for improved ionosphere modelling'. The second author is the recipient of an
7 Australian Research Council (ARC) Federation Fellowship (project number FF0883188). All this support is gratefully
8 acknowledged.

9

10 **REFERENCES**

11

- 12 [1] M. Hernández-Pajares, J. M. Juan, J. Sanz, À. Aragón-Àngel, A. Garc ía-Rigo, D. Salazar, *et al.*, "The ionosphere:
13 effects, GPS modeling and the benefits for space geodetic techniques," *Journal of Geodesy*, vol. 85, pp. 887-907,
14 2011.
- 15 [2] S. Jin and A. Komjathy, "GNSS reflectometry and remote sensing: New objectives and results," *Advances in Space*
16 *Research*, vol. 46, pp. 111-117, 2010.
- 17 [3] N. Jakowski, V. Wilken, S. Schlueter, S. Stankov, and S. Heise, "Ionospheric space weather effects monitored by
18 simultaneous ground and space based GNSS signals," *Journal of atmospheric and solar-terrestrial physics*, vol. 67,
19 pp. 1074-1084, 2005.
- 20 [4] Z. Yiyan, W. Yun, Q. Xuejun, and Z. Xunxie, "Ionospheric anomalies detected by ground-based GPS before the Mw7.
21 9 Wenchuan earthquake of May 12, 2008, China," *Journal of atmospheric and solar-terrestrial physics*, vol. 71, pp.
22 959-966, 2009.
- 23 [5] I. Zakharenkova, I. Shagimuratov, N. Y. Tepenitzina, and A. Krankowski, "Anomalous modification of the
24 ionospheric total electron content prior to the 26 September 2005 Peru earthquake," *Journal of atmospheric and solar-*
25 *terrestrial physics*, vol. 70, pp. 1919-1928, 2008.
- 26 [6] S. Banville, P. Collins, W. Zhang, and R. B. Langley, "Global and Regional Ionospheric Corrections for Faster PPP
27 Convergence," *Navigation*, vol. 61, pp. 115-124, 2014.
- 28 [7] N. Nadarajah and P. Teunissen, "Instantaneous GPS/Galileo/QZSS/SBAS Attitude Determination: A Single -
29 Frequency (L1/E1) Robustness Analysis under Constrained Environments," *Navigation*, vol. 61, pp. 65-75, 2014.

- 1 [8] R. Odolinski, D. Odijk, and P. J. Teunissen, "Combined GPS and BeiDou Instantaneous RTK Positioning,"
2 *Navigation*, vol. 61, pp. 135-148, 2014.
- 3 [9] B. Hofmann-Wellenhof, H. Lichtenegger, and E. Wasle, *GNSS—global navigation satellite systems: GPS, GLONASS,*
4 *Galileo, and more*, : Springer Science & Business Media, 2007.
- 5 [10] Y. Yang, J. Li, A. Wang, J. Xu, H. He, H. Guo, *et al.*, "Preliminary assessment of the navigation and positioning
6 performance of BeiDou regional navigation satellite system," *Science China Earth Sciences*, vol. 57, pp. 144-152,
7 2014.
- 8 [11] J. P. Bartolomé X. Maufroid, I. F. Hernández, J. A. L. Salcedo, and G. S. Granados, "Overview of Galileo System,"
9 in *GALILEO Positioning Technology*, ed: Springer, 2015, pp. 9-33.
- 10 [12] J. Spits and R. Warnant, "Total electron content monitoring using triple frequency GNSS: Results with Giove-A/B
11 data," *Advances in Space Research*, vol. 47, pp. 296-303, 2011.
- 12 [13] J. Spits and R. Warnant, "Total electron content monitoring using triple frequency GNSS data: A three-step
13 approach," *Journal of Atmospheric and Solar-Terrestrial Physics*, vol. 70, pp. 1885-1893, 2008.
- 14 [14] M. Hernández-Pajares, J. Juan, J. Sanz, R. Orus, A. Garcia-Rigo, J. Feltens, *et al.*, "The IGS VTEC maps: a reliable
15 source of ionospheric information since 1998," *Journal of Geodesy*, vol. 83, pp. 263-275, 2009.
- 16 [15] M. Keshin, "A new algorithm for single receiver DCB estimation using IGS TEC maps," *GPS Solutions*, vol. 16, pp.
17 283-292, 2012.
- 18 [16] A. Hauschild, O. Montenbruck, S. Thörlert, S. Erker, M. Meurer, and J. Ashjaee, "A multi-technique approach for
19 characterizing the SVN49 signal anomaly, part 1: receiver tracking and IQ constellation," *GPS solutions*, vol. 16, pp.
20 19-28, 2012.
- 21 [17] A. Hauschild and O. Montenbruck, "A study on the dependency of GNSS pseudorange biases on correlator spacing,"
22 *GPS Solutions*, 2014. DOI. 10.1007/s10291-014-0426-0.
- 23 [18] E. Sardón and N. Zarraoa, "Estimation of total electron content using GPS data: How stable are the differential
24 satellite and receiver instrumental biases?," *Radio Science*, vol. 32, pp. 1899-1910, 1997.
- 25 [19] D. S. Coco, C. Coker, S. R. Dahlke, and J. R. Clynch, "Variability of GPS satellite differential group delay biases,"
26 *Aerospace and Electronic Systems, IEEE Transactions on*, vol. 27, pp. 931-938, 1991.
- 27 [20] O. Montenbruck, A. Hauschild, and P. Steigenberger, "Differential Code Bias Estimation using Multi - GNSS
28 Observations and Global Ionosphere Maps," *Navigation*, vol. 61, pp. 191-201, 2014.
- 29 [21] Z. Li, Y. Yuan, H. Li, J. Ou, and X. Huo, "Two-step method for the determination of the differential code biases of
30 COMPASS satellites," *Journal of Geodesy*, vol. 86, pp. 1059-1076, 2012.

- 1 [22] B. Zhang, J. Ou, Y. Yuan, and Z. Li, "Extraction of line-of-sight ionospheric observables from GPS data using precise
2 point positioning," *Science China Earth Sciences*, vol. 55, pp. 1919-1928, 2012.
- 3 [23] A. Coster, J. Williams, A. Weatherwax, W. Rideout, and D. Herne, "Accuracy of GPS total electron content: GPS
4 receiver bias temperature dependence," *Radio Science*, vol. 48, pp. 190-196, 2013.
- 5 [24] C. Bruyninx, P. Defraigne, and J.-M. Sleewaegen, "Time and frequency transfer using GPS codes and carrier phases:
6 onsite experiments," *GPS Solutions*, vol. 3, pp. 1-10, 1999.
- 7 [25] L. Ciruolo, F. Azpilicueta, C. Brunini, A. Meza, and S. Radicella, "Calibration errors on experimental slant total
8 electron content (TEC) determined with GPS," *Journal of Geodesy*, vol. 81, pp. 111-120, 2007.
- 9 [26] C. Brunini and F. J. Azpilicueta, "Accuracy assessment of the GPS-based slant total electron content," *Journal of*
10 *Geodesy*, vol. 83, pp. 773-785, 2009.
- 11 [27] C. Brunini and F. Azpilicueta, "GPS slant total electron content accuracy using the single layer model under different
12 geomagnetic regions and ionospheric conditions," *Journal of Geodesy*, vol. 84, pp. 293-304, 2010.
- 13 [28] J. F. Conte, F. Azpilicueta, and C. Brunini, "Accuracy assessment of the GPS-TEC calibration constants by means of
14 a simulation technique," *Journal of Geodesy*, vol. 85, pp. 707-714, 2011.
- 15 [29] D. Zhang, H. Shi, Y. Jin, W. Zhang, Y. Hao, and Z. Xiao, "The variation of the estimated GPS instrumental bias and
16 its possible connection with ionospheric variability," *Science China Technological Sciences*, vol. 57, pp. 67-79, 2014.
- 17 [30] D. Zhang, W. Zhang, Q. Li, L. Shi, Y. Hao, and Z. Xiao, "Accuracy analysis of the GPS instrumental bias estimated
18 from observations in middle and low latitudes," *Annales Geophysicae*, vol. 28, pp. 1571-1580, 2010.
- 19 [31] S. Kao, Y. Tu, W. Chen, D. Weng, and S. Ji, "Factors affecting the estimation of GPS receiver instrumental biases,"
20 *Survey Review*, vol. 45, pp. 59-67, 2013.
- 21 [32] P. F. de Bakker, C. C. Tiberius, H. van der Marel, and R. J. van Bree, "Short and zero baseline analysis of GPS L1
22 C/A, L5Q, GIOVE E1B, and E5aQ signals," *GPS solutions*, vol. 16, pp. 53-64, 2012.
- 23 [33] R. Odolinski, P. J. Teunissen, and D. Odijk, "Combined BDS, Galileo, QZSS and GPS single-frequency RTK," *GPS*
24 *Solutions*, vol. 19, pp. 151-163, 2015.
- 25 [34] P. Teunissen, R. Odolinski, and D. Odijk, "Instantaneous BeiDou+ GPS RTK positioning with high cut-off elevation
26 angles," *Journal of Geodesy*, vol. 88, pp. 335-350, 2014.
- 27 [35] N. Nadarajah, P. J. Teunissen, and N. Raziq, "BeiDou inter-satellite-type bias evaluation and calibration for mixed
28 receiver attitude determination," *Sensors*, vol. 13, pp. 9435-9463, 2013.

- 1 [36] P. Teunissen and A. Khodabandeh, "Do GNSS parameters always benefit from integer ambiguity resolution? A PPP-
2 RTK Network Scenario," in *Proceedings of the 27th International Technical Meeting of The Satellite Division of the*
3 *Institute of Navigation (ION GNSS+ 2014)*, Tampa, Florida, September 2014: p. 590-600., pp. 590-600.
- 4 [37] J.-M. Sleewaegen, 2015, Private communication.
- 5 [38] R. Warnant, "Reliability of the TEC computed using GPS measurements—the problem of hardware biases," *Acta*
6 *Geodaetica et Geophysica Hungarica*, vol. 32, pp. 451-459, 1997.
- 7 [39] B.-K. Choi, J.-U. Park, K. M. Roh, and S.-J. Lee, "Comparison of GPS receiver DCB estimation methods using a GPS
8 network," *Earth Planets Space*, vol. 65, pp. 707-711, 2013.

9
10